

RESEARCH

Open Access



Unraveling the association and regulatory role of miR-146b-5p in coronary artery disease

Xiaozhu Ma^{1,2}, Shuai Mei^{1,2}, Yi He^{1,2}, Qidamugai Wuyun^{1,2}, Li Zhou^{1,2}, Ziyang Cai^{1,2}, Qiushi Luo^{1,2}, Yi Wen^{1,2} and Jiangtao Yan^{1,2*}

Abstract

Background Coronary artery disease (CAD), one of the most prevalent cardiovascular diseases, is a critical health issue that affects millions of individuals worldwide. It has been reported that miR-146b-5p exhibited a strong correlation with inflammatory responses and atherosclerosis. However, its association with the incidence and severity of CAD has not been substantiated in a large cohort. In the study, we focus on the expression of miR-146b-5p in peripheral blood mononuclear cells (PBMCs) of patients with CAD and preliminarily investigate its function and underlying mechanism.

Methods and results The study encompassed a total of 452 participants, consisting of 295 patients with CAD and 157 individuals without CAD. Quantitative reverse transcription–polymerase chain reaction (qRT–PCR) was performed to assess miR-146b-5p expression in PBMCs. We found that miR-146b-5p was significantly increased in PBMCs of patients with CAD compared with the control group. Binary logistic regression revealed that miR-146b-5p was associated with CAD. Receiver Operation Characteristic (ROC) analysis showed that the sensitivity and specificity of miR-146b-5p in discriminating CAD patients from non-CAD patients were meaningful. Subsequent subgroup analysis showed that miR-146b-5p was related to the severity of CAD. Furthermore, gain- and loss-of-function experiments in THP-1 cells showed that miR-146b-5p inhibited inflammation, cell proliferation, and migration. Mechanically, miR-146b-5p was involved in the classical NF- κ B inflammatory pathway by directly targeting IKK β .

Conclusion Our study revealed that miR-146b-5p was higher in the PBMCs of CAD patients than non-CAD individuals, and established a correlation between miR-146b-5p and occurrence and severity of CAD. In addition, the inflammatory role of miR-146b-5p is mediated by targeting IKK β .

Keywords miR-146b-5p, Coronary artery disease, Inflammation, IKK β

*Correspondence:

Jiangtao Yan

jtyan@tjh.tjmu.edu.cn

¹Department of Cardiology, Division of Internal Medicine, Tongji Hospital, Tongji Medical College, Huazhong University of Science & Technology, Wuhan, China

²Hubei Key Laboratory of Genetics and Molecular Mechanisms of Cardiological Disorders, Wuhan, China



© The Author(s) 2025. **Open Access** This article is licensed under a Creative Commons Attribution-NonCommercial-NoDerivatives 4.0 International License, which permits any non-commercial use, sharing, distribution and reproduction in any medium or format, as long as you give appropriate credit to the original author(s) and the source, provide a link to the Creative Commons licence, and indicate if you modified the licensed material. You do not have permission under this licence to share adapted material derived from this article or parts of it. The images or other third party material in this article are included in the article's Creative Commons licence, unless indicated otherwise in a credit line to the material. If material is not included in the article's Creative Commons licence and your intended use is not permitted by statutory regulation or exceeds the permitted use, you will need to obtain permission directly from the copyright holder. To view a copy of this licence, visit <http://creativecommons.org/licenses/by-nc-nd/4.0/>.

Introduction

Coronary artery disease (CAD), a prevalent cardiovascular disease, has emerged as the predominant cause of morbidity and mortality across the globe [1]. The latest report indicates that the prevalence of CAD is on the rise, with projections estimating that it will be responsible for approximately 32% of all global deaths by 2035, thereby imposing a heavy economic burden [2].

Atherosclerosis constitutes the principal pathological basis of CAD, with plaque progression facilitating the transition of CAD through various clinical stages, ranging from asymptomatic conditions to stable angina and acute coronary syndrome (ACS) which encompasses unstable angina (UA), ST-elevation myocardial infarction (STEMI), and non-ST-elevation myocardial infarction (NSTEMI). The multifaceted mechanisms of atherosclerosis, such as endothelial dysfunction, inflammation, vascular smooth muscle cell proliferation, and platelet activation, lead to atherosclerotic plaque instability and progression. Notably, inflammatory responses involving the migration of inflammatory factors to the media play a critical role in this process [3, 4]. A recent randomized controlled trial has demonstrated that inflammation, quantified by high-sensitivity C-reactive protein, is a more robust predictor of the risk for future cardiovascular incidents and mortality compared to cholesterol levels determined by low-density lipoprotein [5]. Of note, anti-inflammatory therapy for patients with CAD holds promise for further mitigating adverse cardiovascular events and residual inflammatory risk [6, 7].

MicroRNAs (miRNAs) are endogenous and small non-coding RNAs (about 21 nucleotides) that serve as gene regulators by binding to messenger RNA or the promoters of encoding genes via their complementary sequences [8]. Over the past two decades, the field of miRNA research has experienced rapid development, propelled by advancements in high-throughput sequencing techniques. A growing body of studies found that alterations in miRNA expression can significantly modify the gene expression profiles involved in a wide array of biological processes, thereby playing a pivotal role in the etiology of various human diseases, especially cardiovascular diseases. MiRNAs demonstrate exceptional stability in human biofluids, positioning them as promising biomarkers for disease diagnosis and prognostic evaluation [9]. MiR-451 was reported to improve the differentiation of coronary artery aneurysmal disease (CAAD) from CAD, while miR-328-3p has potential as a biomarker to distinguish patients with CAAD from those with normal coronary arteries [10]. MiR-223, an inflammation-related miRNA, is involved in the progress of atherosclerosis. Nguyen et al. demonstrated that the suppression of miR-223 results in a significant upregulation of cholesterol metabolism and inflammatory signaling, as observed

in both in vivo and in vitro studies. This upregulation is attributed to the global targeting of genes involved in cholesterol efflux and the production of pro-inflammatory cytokines, thereby providing a protective mechanism against atherosclerosis [11]. Additionally, a recent prospective analysis, spanning a 2.8-year follow-up, suggests that incorporating miR-223-3p levels alongside conventional cardiovascular risk factors could enhance the predictive accuracy of cardiovascular event outcomes [12]. Furthermore, a recent study employed Clustered Regularly Interspaced Short Palindromic Repeats (CRISPR) /Cas9 gene editing system targeting miRNA tends to be an effective way for the treatment of thyroid cancer, showing strong prospects for disease therapy based on miRNA [13].

MiR-146b-5p has been implicated in the regulation of inflammatory responses [14]. It suppressed the activation of M1 macrophages, protecting against infection-induced kidney injury [15]. In turn, miR-146b-5p could be induced by M1 polarization and inhibit TNF receptor-associated factor 6 (TRAF6) expression at the post-transcriptional level. Liao et al. observed an upregulation of miR-146b-5p in the infarcted myocardium of both murine and porcine models. Subsequent experiments showed that miR-146b-5p facilitated the transition from fibroblasts to myofibroblasts and disrupted macrophage paracrine signaling by targeting interleukin 1 receptor-associated kinase 1 (IRAK1) and carcinoembryonic antigen-related cell adhesion molecule 1 (CEACAM1) [16]. Our prior research demonstrated that miR-146b-5p was significantly increased in atherosclerotic plaque of ApoE^{-/-} mice and participated in the plaque progress [17]. Mechanistically, miR-146b-5p inhibited vascular smooth muscle cells (VSMCs) proliferation and migration by targeting Bag1 and Mmp16 directly. Of note, a previous study has indicated that circulating miR-146b-5p could serve as a novel biomarker for inflammatory bowel disease [18]. However, the expression of miR-146b-5p in peripheral blood mononuclear cells (PBMCs) of patients with CAD and its association with CAD severity remain unclear. Therefore, we aim to analyze the expression of miR-146b-5p in PBMCs of CAD patients and non-CAD patients as well as establish an association between miR-146b-5p and CAD. In addition, based on the important role of miR-146b-5p in inflammation, we attempted to conduct a preliminary investigation into the functions and mechanisms of miR-146b-5p in the pathogenesis of CAD.

Materials and methods

Study population and sample collection

A total of 452 participants from the COSTIC cohort of Tongji Hospital were included in this study, including 295 patients with CAD and 157 individuals without CAD.

This research conformed to the Declaration of Helsinki guidelines and was approved by the Tongji Hospital Ethics Committee (ID: TJ-C20140716). All participants provided written informed consent. Plasma specimens were collected from individuals over the age of 18 who were admitted to the cardiology department with chest discomfort or dyspnea, all of whom had been subjected to coronary angiography for the confirmation of CAD. Patients with arterial stenosis of over 50% in at least one major coronary artery, as determined by two professional cardiologists following the European Society of Cardiology criteria, were categorized into the CAD group. Individuals presenting with coronary stenosis of less than 50% or with angiographically normal coronary arteries were classified into the non-CAD group. The exclusion criteria were as follows: younger than 18 years of age, patients with heart failure, severe hepatic or renal dysfunction, patients on any anti-inflammatory modulators or with myocarditis, autoimmune diseases, infectious disease, patients with uncontrolled bronchial asthma and chronic obstructive pulmonary disease, oncological disease, or unwillingness to provide written consent. Demographic data and clinical characteristics were collected from all groups. Gensini score was calculated by assigning a value to each coronary segment according to the degree of stenosis [19]. The peripheral blood samples were collected during the coronary angiography procedure and kept at 4°C temporarily. The primary outcomes of this study are the association between miR-146b-5p and the occurrence and severity of CAD. The secondary outcome is the association between miR-146b-5p and the risk factors of CAD.

The establishment of animal models

The C57BL/6 mice was purchased from GemPharmatech Co., Ltd. (Jiangsu, China) and the construction of pathological models was described in a previous study of S.M [20]. Briefly, the right carotid artery of 8-week-old male mice was meticulously isolated and visualized under a microscope after anesthesia. Subsequently, the internal and external carotid arteries were secured with 7–0 silk sutures, and the proximal common carotid artery was occluded using a vascular clamp. Importantly, a slipknot was placed around the internal carotid artery. A flexible guidewire with 0.4 mm in diameter was inserted into the common carotid artery and maneuvered three times to induce injury. After repositioning the guidewire, the proximal common carotid artery was ligated. The incision was closed with 5–0 surgical silk sutures. The mice were sacrificed 28 days post-surgery for further analysis. All mice we used were euthanized by intraperitoneal injection of pentobarbital Sodium (Sigma, USA) at 50 mg/kg. The artery tissues of mice utilized in this study were obtained from our prior research, which adhered

to the Institutional Animal Care and Use Committee (IACUC) protocols and granted approval by the Animal Research Committee's Ethics Board of Tongji Medical College, Huazhong University of Science and Technology ([2022] IACUC Number 3836).

PBMC isolation and RNA extraction

PBMCs are a heterogeneous population of immune cells found in the peripheral blood, which play a crucial role in the immune system. PBMCs were extracted from 8 mL whole blood within 6 h of collection. PBMCs were separated according to the Ficoll-Hypaque density-gradient centrifugation technique as previously described [21]. In brief, the venous blood samples were subjected to centrifugation at a speed of 3000 rpm for 8 min and the supernatant was removed. The remaining samples were diluted with an equal amount of PBS and then added gently into peripheral blood lymphocyte separation fluid (Yes service biotech, China). The samples were centrifuged differentially at 500 g for 30 min. After that, cell clumps in the middle layer were collected into a new centrifuge tube followed by washed with PBS twice.

Total RNA was extracted from purified PBMCs utilizing the RNA isolater Total RNA Extraction Reagent (Vazyme, China) according to the manufacturer's instructions. To detect miR-146b-5p level in the carotid arteries and aortas of animal models, we removed the frozen vascular tissues and placed them into grinding tubes containing sterilized zirconium oxide grinding beads. We then added 1 ml of TRIzol reagent and performed low-temperature grinding with 120 Hz for 2 min. The subsequent RNA extraction steps were same as those used for cells. RNA concentration and integrity were analyzed using a NanoDrop 1000 Spectrophotometer (Thermo Scientific, USA), prior to storage at -80 °C.

cDNA synthesis and qPCR assays

1 µg of RNA was used for reverse transcriptase with the HiScript II 1st Strand cDNA Synthesis Kit (Vazyme, China) following the manufacturer's instructions. Subsequently, qPCR was conducted with SYBR Green Master Mix (Vazyme, China). The miRNA-specific primers were crafted and purchased from Riobio Co., Ltd (Guangzhou, China). The primers of other molecules were listed in Table S1. The expression of miRNAs and mRNA was calculated by $2^{-\Delta\Delta C_t}$ and U6 or GAPDH was regarded as internal control for data normalization.

Enzyme-linked immunosorbent assay (ELISA)

ELISA is a widely utilized immunological technique for the detection and quantification of specific substances, such as peptides, proteins, and hormones. This method is based on the specific binding of an antibody to its corresponding antigen. Concentrations of TNF- α , IL-6,

and IL-1 β within THP-1 cells were determined utilizing a standard ELISA kit (Abclonal, China) according to the provided protocol. Briefly, the wells of antibody-coated plate were washed three times with washing buffer, followed by the addition of standards or samples and incubation at 37 °C for 2 h. After washing, the plate was incubated successively with biotinylated detection antibody working solution, streptavidin-horseradish peroxidase (HRP) working solution, TMB substrate, and stop buffer. Finally, the expression of three molecules was measured by recording the absorbance at 450 nm using a plate reader.

Cell culture and transfection

Human monocyte cell line THP-1 and 293T cells were from American Type Culture Collection. They were maintained in Roswell Park Memorial Institute medium 1640 (Gibco, USA) and Dulbecco's Modified Eagle's Medium (Gibco, USA) containing 10% FBS (Gibco, USA), respectively. All cells were cultured in an incubator at 37 °C with 5% CO₂. Custom-designed miR-146b-5p mimics and antagomirs, along with their respective negative control oligos, were synthesized by Guangzhou RiboBio Co., Ltd. THP-1 cells plated in 6-well plates and transfected with HiPerFect Transfection Reagent (Univ, China) following the manufacturer's instructions. For subsequent analysis, cells were collected 48 h post-transfection.

Western blot

The protein concentrations of the samples were ascertained employing the BCA protein assay method. Denatured samples were subjected to sodium dodecyl sulfate-polyacrylamide gel electrophoresis (SDS-PAGE). Subsequent to electrophoresis, the proteins were transferred onto a polyvinylidene fluoride (PVDF) membrane. The membrane was then incubated with primary antibodies specific to the proteins of interest at 4 °C overnight after being blocked. The primary antibodies utilized in this study are TNF- α , MCP-1, CCND1, IKKB, and β -actin. Details regarding these antibodies are presented in Table S2. Proceeding to day 2, the membrane was washed and incubated with corresponding secondary antibodies. At last, the protein bands of interest were quantified and analyzed through a chemiluminescence image.

CCK8 assay

The cell proliferative capacity was evaluated by Cell Counting Kit-8 (Yeasen, China). Briefly, the cells with good state were incubated in CCK8 reagent which was mixed with DMEM complete medium at 37 °C CO₂ incubator for 2 h. The absorbance of cells was measured with 450 nm at different points after transfection.

5-ethynyl-2'-deoxyuridine (EdU) assay

EdU assay was performed to assess cell proliferation according to the cell-Light™ EdU Apollo In Vitro Kit (RiboBio, China). THP-1 cells were incubated with 50 μ m EdU buffer for 2 h. Next, the cells were fixed in 4% paraformaldehyde (PFA) for 20 min at ambient temp. Then glycine was used to neutralize formaldehyde. The cells were then treated with 0.5% Triton X-100 for about 10 min for permeabilization. After that, the cells are incubated with the Apollo staining reagent that has been prepared and used under conditions of room temperature and protected from light. The nucleus was stained with hoechst and the results were analyzed via an inverted fluorescence microscope.

Wound healing assay

Wound healing assay was performed to evaluate the cell migration. THP-1 cells were induced to adhere by phorbol 12-myristate 13-acetate (PMA) for 24 h, then a cross line was drawn in the six-well plate with a sterile pipette tip, followed by washing twice with PBS. The cells were incubated by complete culture medium without phenol red. At regular intervals, the scratch area was observed under an ordinary light microscope to assess the migration of cells into the scratch.

Dual-luciferase assay

The binding between miR-146b-5p and IKKB 3' untranslated regions (3'UTR) was assessed by Dual-Luciferase® Reporter Assay System (Promega, USA). The 3'UTR of IKKB was inserted into a pGL3-promoter vector and co-transfected with miR-146b-5p mimics or negative controls. After transfection for 48 h, the cells were lysed with passive lysis buffer and the fluorescence intensity was measured by dual-luciferase assay.

RNA binding protein immunoprecipitation assay, RIP

RIP experiments were conducted to assess the interaction between miR-146b-5p and Argonaute 2 (AGO2) protein. Initially, protein A/G magnetic beads (MCE, USA) were equilibrated to room temperature and then washed with 100 μ L of wash buffer, composed of KCl, Tris-Cl, EDTA, NP40, and DEPC-treated water. The beads were subsequently incubated with AGO primary antibody at room temperature with rotational mixing for 1 h. Cells were harvested and lysed using IP lysate buffer added with a protease inhibitor cocktail (Abclonal, China) and RNase inhibitor (Abclonal, China) to preserve the integrity of cellular components. The lysate was then mixed with the antibody-coated beads and incubated overnight at 4 °C with rotational mixing in RIP IP buffer. On day 2, the beads were thoroughly washed three times with wash buffer prior to RNA extraction.

Fluorescence in situ hybridization, FISH

Paraffin-embedded vascular tissue sections were placed on glass slides and baked at 60 °C for 1 h. The slides were then deparaffinized by immersing in xylene for 10 min, repeated twice with fresh xylene, followed by dehydration in different concentrations of ethanol. Subsequently, antigen retrieval was performed by placing the slides in a sodium citrate buffer under high-temperature conditions. Upon reaching ambient temperature, the sections were subjected to pre-hybridization with 3% BSA in 4 x SSC at 55 °C for 20 min. The miR-146b-5p probe was then added for hybridization at 55 °C for 1 h. Following hybridization, the sections were washed and treated with 3% H₂O₂ for 20 min to block endogenous peroxidase activity. The sections were then washed three times with TN buffer, blocked with TNB buffer for 30 min, and incubated with a digoxigenin-conjugated primary antibody for 30 min. After washing three times with TNT buffer, the sections were incubated with TSA solution in the dark for 10 min. Subsequently, the sections were incubated with a CD68 primary antibody (1:100 in PBS) overnight at 4 °C in the dark. The next day, the sections were washed with PBS and incubated with a fluorescent secondary antibody. Nuclei were stained with DAPI, and the sections were mounted with an anti-fade mounting medium. Finally, the expression of miR-146b-5p was observed under a fluorescence microscope.

Statistical analysis

Statistical analyses and figure preparation were performed using SPSS software version 24.0 for Windows (SPSS Inc, USA) and GraphPad Prism 8.0 (GraphPad Software, USA). Kolmogorov–Smirnov test was performed used to analyze the normality of distribution. Continuous variables were represented as mean ± standard deviation (SD), whereas categorical variables were described as medians and interquartile ranges. Comparisons between two groups were conducted using either the Mann-Whitney U test or the two-sided Student's t-test based on the normality of the data. Kruskal-Wallis test followed by Dunn's post-hoc test were used for comparison of miR-145b-5p among three groups. The Chi-square test was utilized to compare categorical variables. Binary logistic regression was employed to analyze the correlation between miR-145b-5p and CAD. Stepwise logistic regression was performed to adjust underlying confounders, including gender, smoking status, diabetic mellitus, hypertension, HDL-C, eGFR. Spearman correlation analysis was used for correlation between miR-145b-5p and the Gensini score and traditional risk factors of CAD. The receiver operating characteristic (ROC) curve analysis was used to assess the discriminatory power of miR-145b-5p, and the optimal threshold for candidate miRNA biomarkers was determined using

Youden's method. In all analyses, a *p*-value of less than 0.05 was deemed to indicate statistical significance.

Sample size

Prior to the study, a power analysis was conducted to determine the appropriate sample size. Based on an effect size of 0.5, a significance level of 0.05, and a desired power of 0.9, it was determined that a minimum of 90 participants per group would be required. After finalizing the inclusion criteria, the study enrolled 159 participants in the control group and 295 patients with CAD. A post-hoc power analysis was then performed using the actual sample sizes (N₁ = 157 for controls and N₂ = 295 for CAD patients), with the effect size set at 0.5 and the significance level at 0.05. The analysis revealed a power of 99.85%, indicating that our study is more than adequately powered to detect meaningful differences in miR-145b-5p expression level between the groups. The power analysis was conducted using G*Power software 3.1.9.7.

Results

Baseline and clinical characteristics of the study population

In this study, we included a total of 452 patients, comprising 295 individuals with CAD and 157 without. The baseline characteristics and demographics of the study subjects were shown in Table 1. There were no statistically significant differences in age, BMI, blood pressure, total cholesterol, triglycerides, low-density lipoprotein cholesterol level, alanine aminotransferase, creatinine, blood count, and a history of dyslipidemia, whereas the CAD group exhibited a significantly higher proportion of male patients. Notably, this gender disparity within the cohorts corresponded with worldwide statistics regarding gender-related frequency of CAD [22]. Also, traditional risk factors of CAD, including smoking, diabetic mellitus, and hypertension, as well as high-density lipoprotein cholesterol (HDL-C), glucose, and estimated glomerular filtration rate (eGFR) value differed between the two groups. In addition, there was no statistically significant difference observed in the left ventricular ejection fraction.

The expression of miR-146b-5p in PBMCs of the study groups

As depicted in Fig. 1A, the qRT-PCR result indicated a significant increase in miR-146b-5p expression was observed in PBMCs among patients with CAD compared to the non-CAD group (Median: 1.723 vs. 1.101, *p* < 0.001). Upon conducting a subgroup analysis stratified by gender, the results indicated that the upregulation trend of miRNA in patients with CAD was consistently observed in both male and female cohorts (male: *Z* = -5.155, *p* < 0.001; female: *Z* = -4.605, *p* < 0.001).

Table 1 Baseline characteristics of the study participants

Variable	Non-CAD n = 157	CAD n = 295	Pvalue
Male (%)	81(51.6)	204(69.2)	< 0.001
Female (%)	76(48.4)	91(30.8)	< 0.001
Age (years)	58.43 ± 9.90	60.04 ± 9.87	0.098
BMI (kg/m ²)	23.8 ± 3.45	24.12 ± 3.23	0.332
Smoking (%)	42 (26.8)	114 (38.6)	0.011
Diabetic mellitus (%)	28 (17.8)	88 (29.8)	0.005
Hypertension (%)	68 (43.6)	167 (56.6)	0.008
Dyslipidemia (%)	126 (80.3)	234 (79.3)	0.815
SBP (mmHg)	128.62 ± 21.95	127.42 ± 64.37	0.822
DBP (mmHg)	80.72 ± 12.5	79.72 ± 12.02	0.406
TC (mg/dL)	3.88 ± 0.86	3.72 ± 1.15	0.113
TG (mg/dL)	1.73 ± 1.41	1.97 ± 1.53	0.119
LDL-C(mg/dL)	2.17 ± 0.89	2.13 ± 1.02	0.672
HDL-C(mg/dL)	1.1 ± 0.26	1.01 ± 0.26	< 0.001
Glucose (mmol/L)	6.2 ± 2.15	7.29 ± 2.8	< 0.001
ALT (U/L)	21.64 ± 14.82	27.11 ± 64.14	0.302
Creatinine (umol/L)	84.15 ± 87.14	98.8 ± 102.144	0.136
eGFR (ml/min/1.73 m ²)	88.62 ± 23.04	80.18 ± 39.18	0.016
WBC (*10 ⁹ /L)	6.54 ± 2.5	6.93 ± 2.71	0.134
Ejection fraction (%)	49.01 ± 7.06	48.92 ± 7.03	0.084

The data are expressed as a mean ± SD (continuous data) or as frequencies (%) (categorical data). CAD, Coronary artery disease; BMI: Body Mass Index; SBP: systolic blood pressure; DBP: diastolic blood pressure; TC: total cholesterol; TG: triglycerides; LDL-C: low-density lipoprotein cholesterol; HDL-C: high-density lipoprotein cholesterol; ALT: alanine aminotransferase; eGFR: estimated glomerular filtration rate; WBC: white blood cell

Association between miR-146b-5p in PBMCs and the occurrence of CAD

There was no significant correlation between miR-146b-5p and traditional risk factors of CAD, including smoking, hypertension, dyslipidemia and diabetes ($r = 0.034$ and $p = 0.476$, $r = -0.026$ and $p = 0.587$, $r = -0.027$ and $p = 0.563$, $r = -0.033$ and $p = 0.489$, respectively). To further elucidate the association between miR-146b-5p and the risk of developing CAD, we performed both univariate and multivariate logistic regression analyses, the results of which were presented in Tables 2 and 3, respectively. The univariate logistic regression was conducted based on the clinical parameters that exhibited differential expression between the two groups, including gender, smoking status, diabetic mellitus, hypertension, HDL-C, eGFR, and miR-146b-5p. In the multivariate logistic regression analysis, variables with a P -value less than 0.05 in the univariate analysis were included. Multivariate logistic regression analysis further indicated that male gender and increased miR-146b-5p were associated with a higher risk of CAD ($p < 0.001$), whereas HDL-C served as a protective factor against the development of CAD. Furthermore, ROC analysis based on this model demonstrated satisfactory predictive efficacy, with sensitivity and specificity values of 65.2% and 70.5%, respectively.

The area under the curve (AUC) was 0.74 (0.692–0.787, $p = 0.024$), as demonstrated in Fig. 1B.

Association between miR-146b-5p and the severity of CAD
Considering that miR-146b-5p is elevated in PBMCs of patients with CAD and is closely related to cardiac and vascular inflammation, we wonder whether there is a difference in miR-146b-5p expression among patients with different severities of CAD. Firstly, we categorized the CAD patients into three subgroups according to the type of CAD. The result showed that miR-146b-5p expression was higher in PBMCs of patients in the unstable angina group than those in the stable angina group ($p = 0.016$). However, no significant difference was observed when compared to the myocardial infarction group (Fig. 1C). Furthermore, the severity of CAD can be partially assessed by the number of diseased coronary arteries. Consequently, we analyzed the differential expression of miR-146b-5p level between patients with single-vessel CAD and those with multi-vessel CAD. The results indicated that patients with multi-vessel disease exhibited significantly elevated miR-146b-5p levels in their PBMCs (Fig. 1D, $p = 0.013$). Additionally, Spearman correlation analysis identified a weak positive correlation between the Gensini score and miR-146b-5p levels (Fig. 1E).

miR-146b-5p was involved in the pathophysiological processes of CAD

Previous research indicates that miR-146b-5p responds to lipopolysaccharides or TNF- α stimulation [23]. To explore the association between miR-146b-5p and inflammation, two established animal models related to CAD, including the carotid artery injury model and the atherosclerosis model, were utilized to detect the expression of miR-146b-5p. QRT-PCR results demonstrated that miR-146b-5p was significantly upregulated in the injured carotid artery and the aorta of high-fat diet-fed ApoE^{-/-} mice (Fig. 2A and C). In addition, the inflammation response was dramatically activated, as evidenced by an increase in CD68-positive cells by FISH. The level of miR-146b-5p was also increased in macrophages, as detected by FISH (Fig. 2B and D). These results indicated that miR-146b-5p may play a significant role in CAD.

miR-146b-5p negatively regulated the inflammation and proliferation in macrophages

To elucidate the role of miR-146b-5p in the regulation of inflammation and macrophage proliferation, we transfected THP-1 cells with miR-146b-5p mimics or a negative control mimic (mimic-NC) and confirmed the effective overexpression of miR-146b-5p by qRT-PCR (Fig. 3A). Subsequently, by qRT-PCR and western blot, we observed that the level of inflammation-related cytokines, such as TNF α , IL-1 β , and IL-6, was reduced

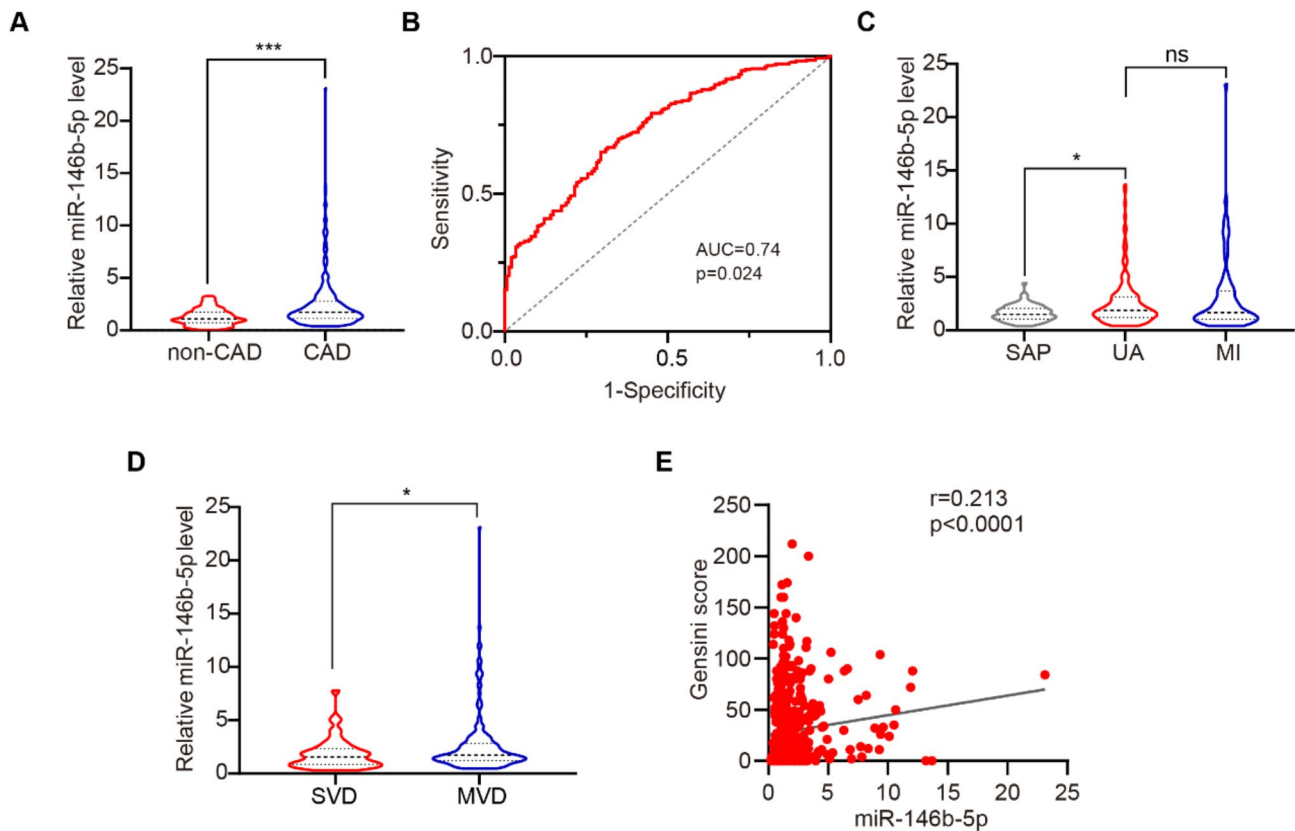


Fig. 1 The expression of miR-146b-5p in PBMCs of the study participants and its association with CAD. **(A)** Comparison for the miR-146b-5p level in CAD patients with non-CAD individuals. The data were normalized to U6. The dashed lines in violin plot represents median (middle) and interquartile ranges (top and bottom). Mann-Whitney U test was used. *** $p < 0.001$. **(B)** ROC curve of the model defining the risk of CAD. AUC = area under the curve. **(C)** Comparison for the miR-146b-5p level among different types of CAD. Kruskal-Wallis test followed by Dunn's post-hoc test was used. **(D)** The expression levels of miR-146b-5p were compared between patients with single-vessel disease (SVD) and those with multi-vessel disease (MVD). Mann-Whitney U test was used. **(E)** The correlation between miR-146b-5p and Gensini score by the Spearman correlation analysis. * $p < 0.05$, ns-not significant

Table 2 Univariate logistic regression analysis for CAD patients

Variable	OR	95%CI	Pvalue
Male	2.103	1.412–3.134	<0.001
Female	2.103	1.412–3.134	<0.001
Smoking	1.725	1.129–2.635	0.012
Diabetic mellitus (%)	1.959	1.213–3.161	0.006
Hypertension (%)	1.688	1.142–2.497	0.009
HDL-C	0.252	0.118–0.541	<0.001
eGFR	0.992	0.982–0.999	0.031
miR-146b-5p	2.088	1.635–2.666	<0.001

OR: odds ratio; CI: confidence interval. HDL-C: high-density lipoprotein cholesterol; eGFR: estimated glomerular filtration rate

Table 3 Multivariate logistic regression analysis for CAD patients

Variable	OR	95%CI	Pvalue
Male	1.81	1.044–3.136	0.034
Female	1.81	1.044–3.136	0.034
Smoking	1.173	0.669–2.059	0.578
Diabetic mellitus (%)	1.566	0.903–2.715	0.11
Hypertension (%)	1.509	0.959–2.374	0.075
HDL-C	0.34	0.139–0.831	0.018
eGFR	0.996	0.989–1.002	0.168
miR-146b-5p	2.271	1.723–2.993	<0.001

OR: odds ratio; CI: confidence interval. HDL-C: high-density lipoprotein cholesterol; eGFR: estimated glomerular filtration rate

in response to miR-146b-5p overexpression (Fig. 3B-C). Consistent results were also observed in the enzyme-linked immunosorbent assay (Fig. 3D-F). In addition, the proliferation-related protein Cyclin D1 (CCND1) was significantly repressed likewise with miR-146b-5p mimics (Fig. 3G). Both CCK-8 and EdU assays implied that the proliferation ability of macrophage was declined when miR-146b-5p was overexpressed (Fig. 3H&I). The monolayer wound-healing assay indicated miR-146b-5p

restrained the migration of THP-1 cells (Fig. 3J). Furthermore, the opposite effects were observed with miR-146b-5p deficiency (Fig. 4). Collectively, these data suggested that miR-146b-5p negatively regulated inflammation and suppressed the proliferation and migration capacity in vitro.

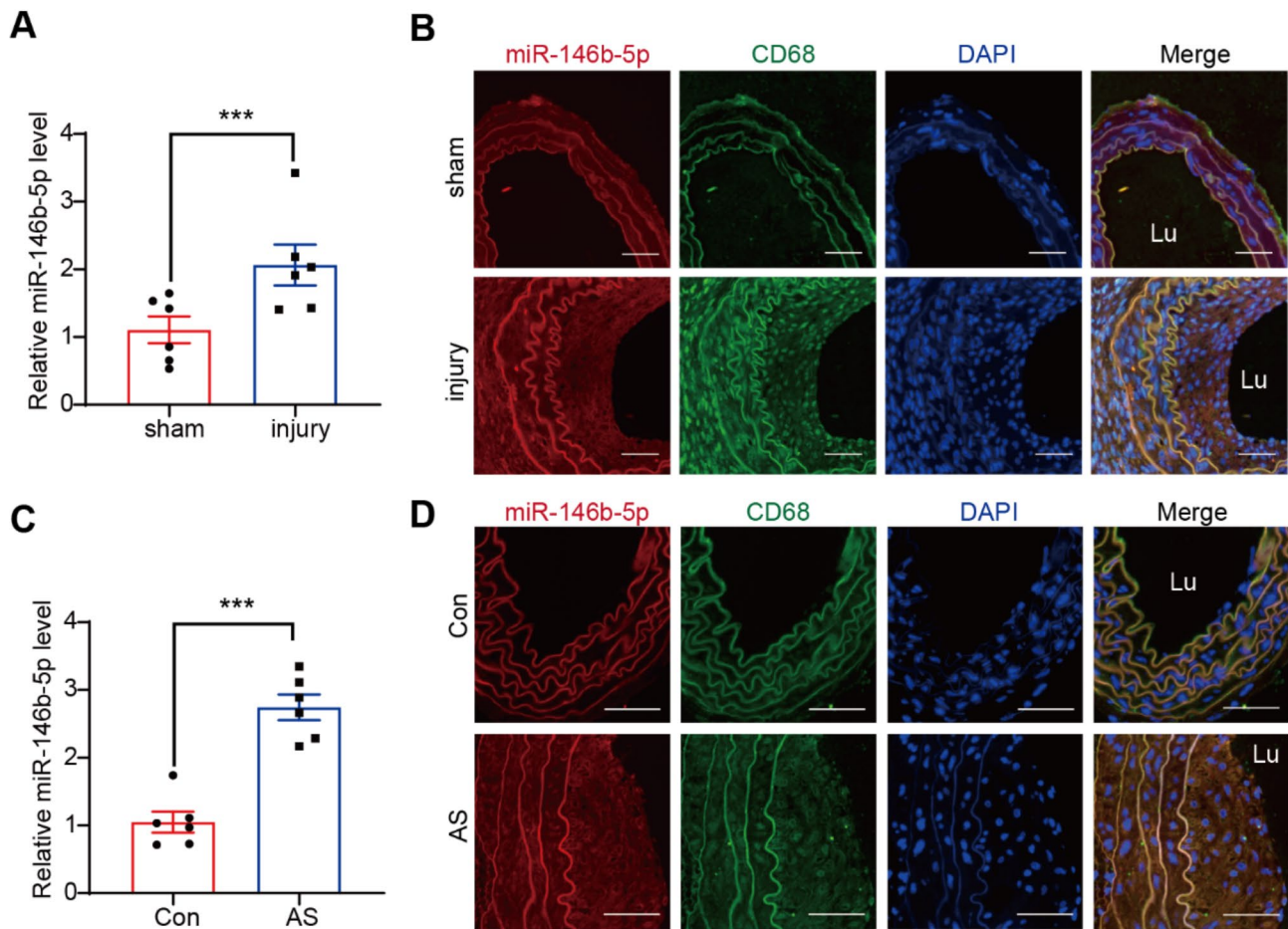


Fig. 2 The miR-146b-5p expression was increased in two inflammation-related models. **(A-B)** The expression of miR-146b-5p in injured artery detected by qRT-PCR **(A)** and FISH **(B)**. CD68 as the marker of macrophages. Scale bar = 25 μ m. **(C-D)** The expression of miR-146b-5p in atherosclerotic plaque detected by qRT-PCR **(C)** and FISH **(D)**. CD68 as the marker of macrophages. Scale bar = 50 μ m. Student t test was used. *** p < 0.001

miR-146b-5p ameliorated inflammation progression by directly targeting IKK β

To further elucidate the mechanism by which miR-146b-5p serves as an anti-inflammatory factor, the miR-Walk 2.0 website was used to predict the target genes of miR-146b-5p [24]. Kyoto Encyclopedia of Genes and Genomes (KEGG) analysis indicated the potential target genes were enriched in inflammation-related pathways, such as Th17 cell differentiation and leukocyte transendothelial migration (Fig. 5A). Furthermore, we discovered that I κ B kinase beta (IKK β), a critical factor of the NF- κ B pathway, as a potential target of miR-146b-5p, with the binding sites demonstrating strong conservation across species (Fig. 5B). IKK β is a crucial regulatory kinase involved in the activation of the inflammation response [25]. Therefore, it was chosen for further investigation. The overexpression of miR-146b-5p by miR-146b-5p mimics significantly inhibits the expression of IKK β at mRNA level and protein level, whereas IKK β was increased when miR-146b-5p was knocked down by miR-146b-5p antagomir in THP-1 cells (Fig. 5C-F). It has been

reported that AGO2 binds to miRNA to form the RNA-induced silencing complex (RISC), which can recognize and bind to complementary sequence of target mRNA [26]. Therefore, we wondered whether Ago2 could mediate the function of miR-146b-5p on IKK β mRNA, and then performed AGO2-RIP assay in THP-1 cells. The result demonstrated that the mRNA of IKK β was significantly enriched by the AGO2 antibody compared with the IgG antibody (Fig. 5G). To further confirm the direct interaction, we conducted a dual-luciferase reporter assay, and found that miR-146b-5p could directly bind to 3'UTR of IKK β in THP-1 cells (Fig. 5H). These suggested miR-146b-5p bound to IKK β , thereby playing a role in the inflammatory response.

Discussion

In this study, we have identified that miR-146b-5p is upregulated in PBMCs of patients with CAD and associated with an increased risk of developing CAD. Subgroup analysis reveals a certain correlation between miR-146b-5p and the severity of CAD. In vitro, miR-146b-5p

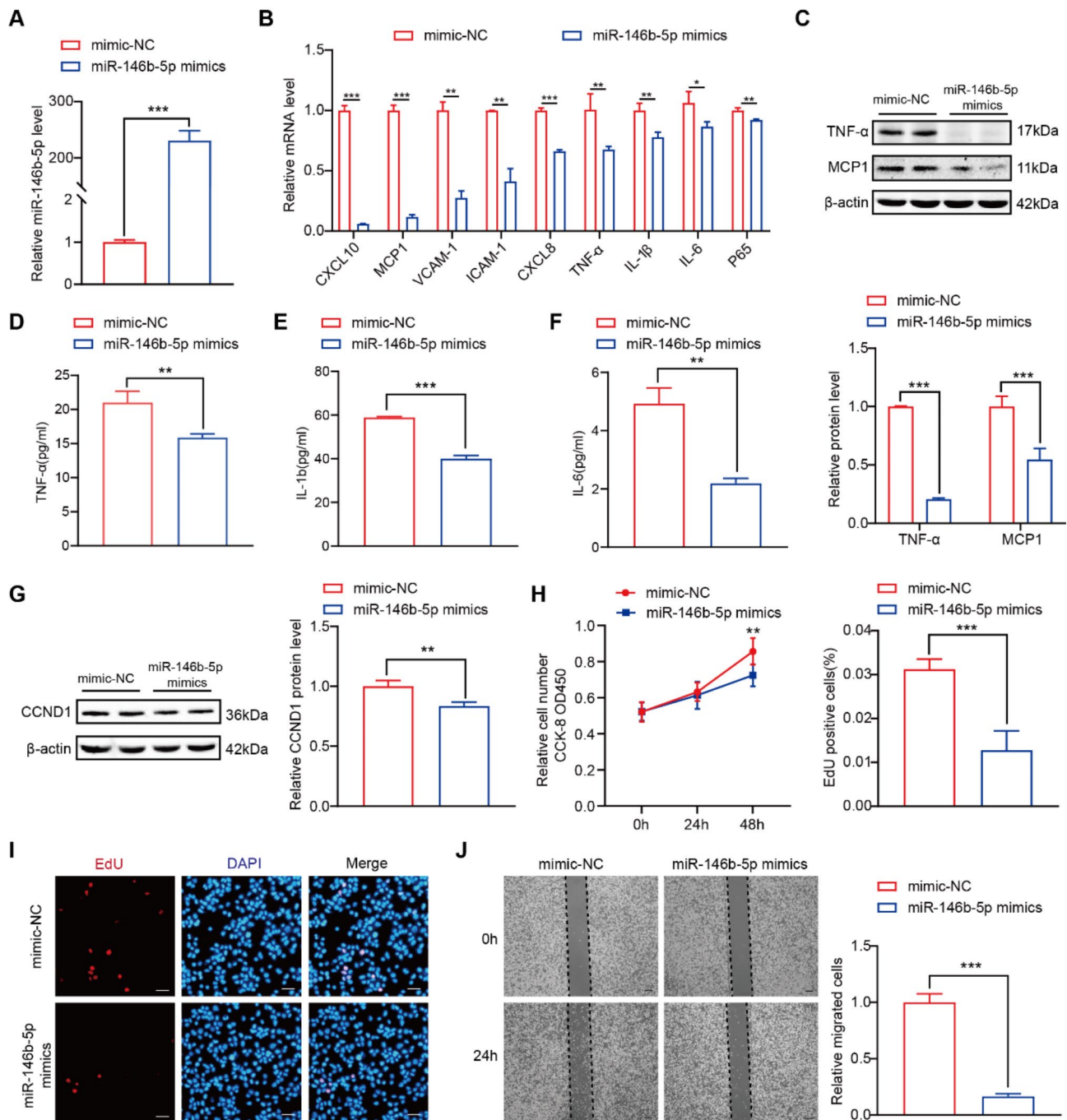


Fig. 3 miR-146b-5p overexpression inhibited the inflammation, proliferation and migration in vitro. **(A)** miR-146b-5p was overexpressed through mimics in THP-1 cells. **(B)** Inflammatory cytokines were assessed by qRT-PCR with miR-146b-5p overexpression. **(C)** The expression of inflammatory related markers detected by western blot. **(D-F)** The expression of TNF-α **(D)**, IL-1β **(E)**, and IL-6 **(F)** in the supernatant of THP-1 cells detected by ELISA. **(G)** The expression of proliferation-related markers detected by western blot. **(H-I)** The proliferative ability of THP-1 cells was evaluated by CCK-8 assay **(H)** and EdU assay **(I)**, scale bar = 50 μm. **(J)** The migratory ability of THP-1 cells was assessed by the wound-healing assay. Scale bar = 200 μm. Student t test was used. ****p* < 0.001, ***p* < 0.01, **p* < 0.05

suppresses macrophage inflammation, proliferation, and migration. Mechanically, miR-146b-5p binds to the 3'UTR of IKKβ and inhibits its expression, thereby participating in the modulation of the inflammatory response.

There are two subtypes of the miR-146 family, including miR-146a and miR-146b. These subtypes are distinguished by their distinct genomic locations and differ by only two nucleotides at their 3' ends. A range of studies have shown that miR-146b is mainly involved in

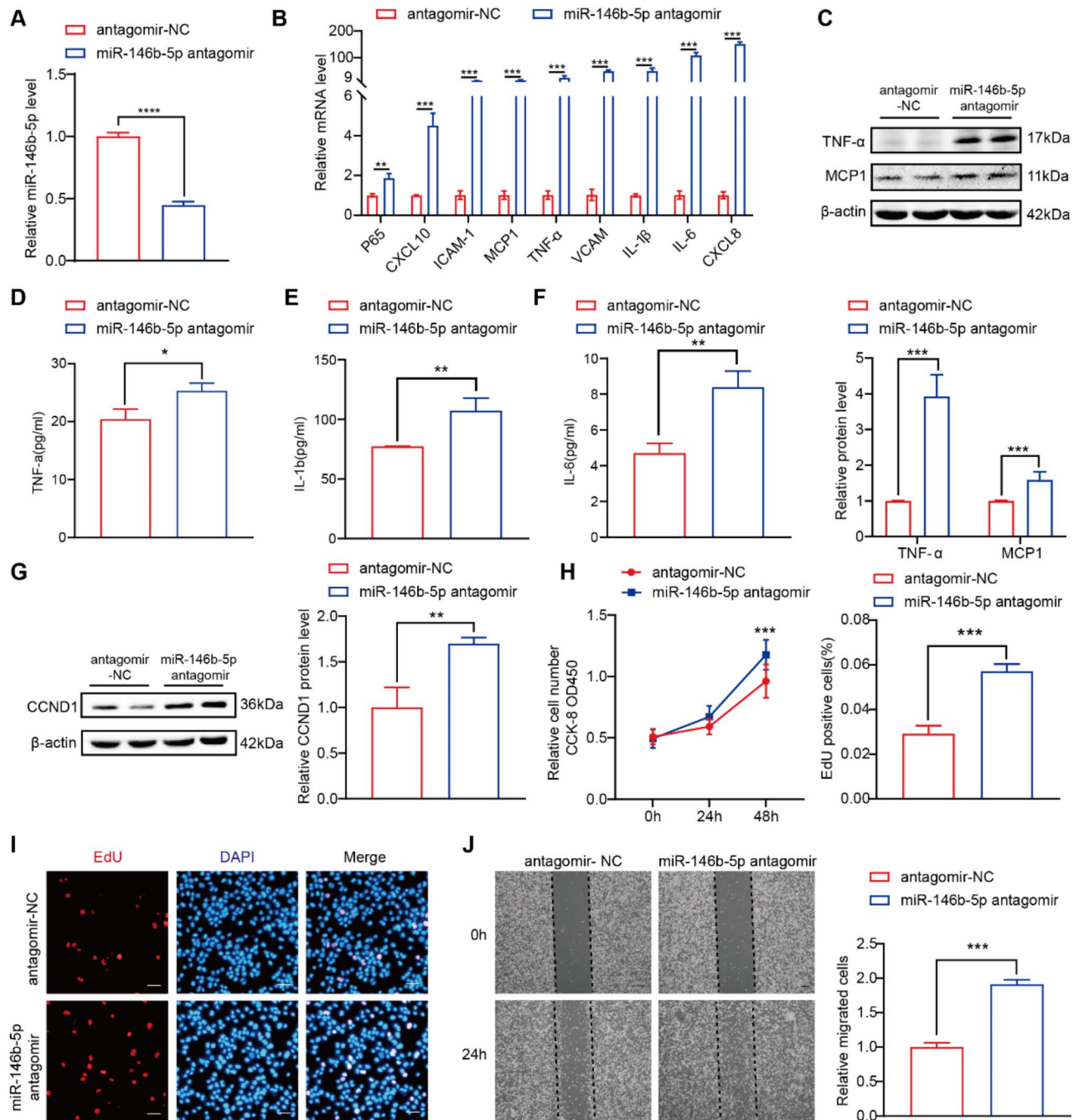


Fig. 4 miR-146b-5p knockdown exacerbate inhibited the inflammation, proliferation and migration in vitro. **(A)** miR-146b-5p was inhibited via antagomir transfection in THP-1 cells. **(B)** Inflammatory cytokines were assessed by qRT-PCR with miR-146b-5p knockdown. **(C)** The expression of inflammatory related markers detected by western blot. **(D-F)** The expression of TNF-α **(D)**, IL-1β **(E)**, and IL-6 **(F)** in the supernatant of THP-1 cells by ELISA. **(G)** The expression of proliferation-related markers detected by western blot. **(H-I)** The proliferative ability of THP-1 cells was evaluated by CCK-8 assay **(H)** and EdU assay **(I)**, scale bar = 50 μm. **(J)** The migratory ability of THP-1 cells was assessed by the wound-healing assay. Scale bar = 200 μm. Student t test was used. ****p* < 0.001, ***p* < 0.01, **p* < 0.05

inflammatory response and cancers [27, 28]. Chang et al. found that miR-146-5p significantly suppresses endothelial cell migration by binding to the 3'UTR of RhoA, thereby participating in angiogenesis and vascular repair [29]. Our previous research has elucidated the critical

function of miR-146b-5p in the proliferation and migration of VSMCs, suggesting the association between miR-146b-5p and atherosclerosis. Herein, we further confirmed the increased expression of miR-146b-5p in PBMCs of patients with CAD and found the positive

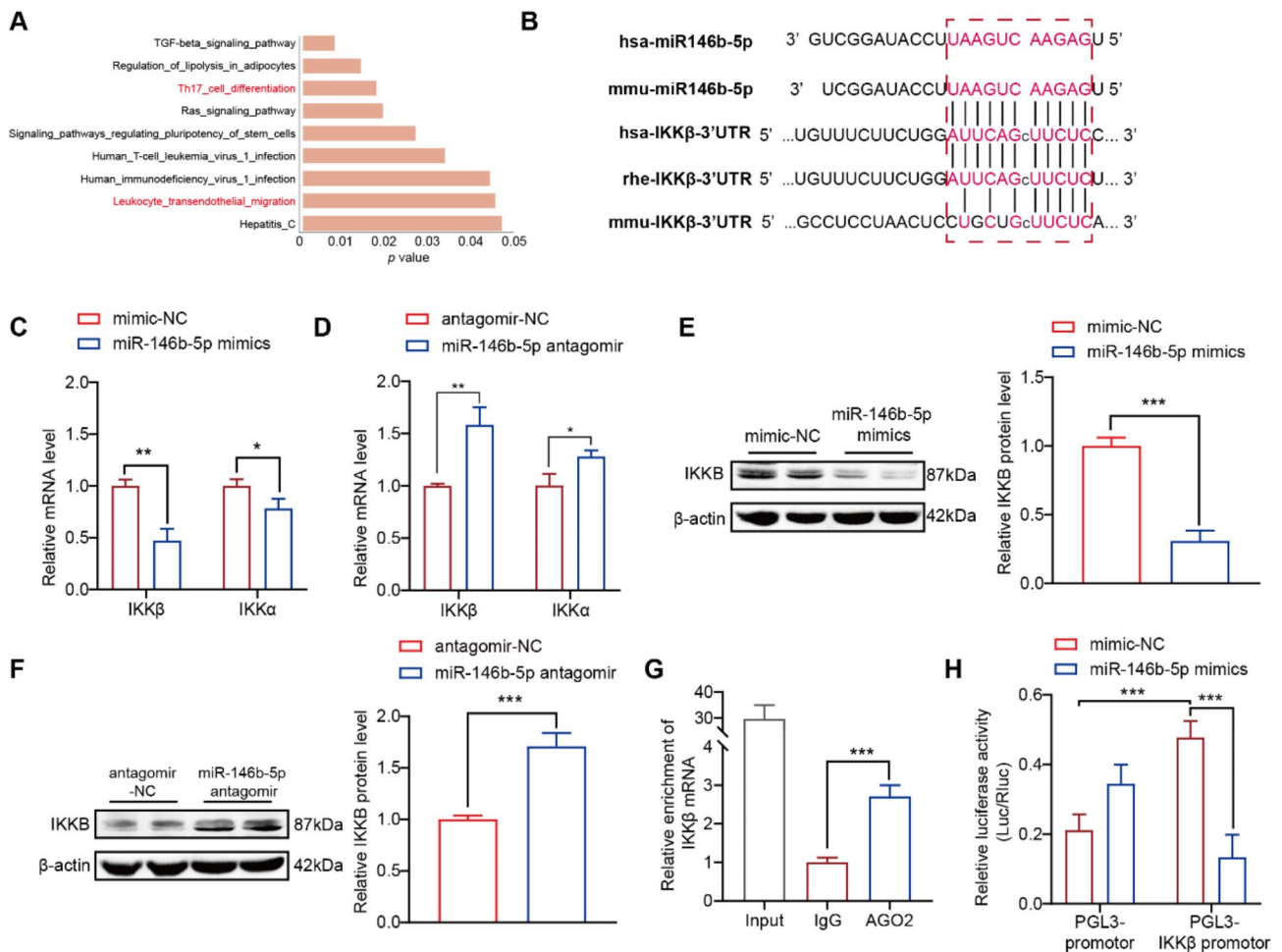


Fig. 5 miR-146b-5p was involved in the inflammation by targeting IKKB. **(A)** KEGG pathway analysis to identify the potential targets of miR-146b-5p from miRWalk 2.0 database. **(B)** The predicted complementary sequences between miR-146b-5p and the 3'UTR of IKKB of different species. **(C-D)** the mRNA expression of IKKα and IKKβ with miR-146b-5p overexpression **(C)** and knockdown **(D)**. **(E-F)** the expression of IKKα and IKKβ with miR-146b-5p overexpression **(E)** and knockdown **(F)** detected by western blot. **(G)** RNA binding protein immunoprecipitation (RIP) assay showed Ago2 bound to mRNA of IKKB. **(H)** The luciferase assay showed the interaction between miR-146b-5p and the 3'UTR of IKKB. Student t test was used for C-F. One-way ANOVA was used in G. Two-way ANOVA was used in H. *** $p < 0.001$, ** $p < 0.01$, * $p < 0.05$

correlation between miR-146b-5p and the occurrence of CAD. The result is consistent with some previous studies, which showed that miR-146b level was higher in the plasma of patients with CAD than in the non-CAD group in small sample population [23]. Liao et al. discovered a significant upregulation of plasma miR-146b-5p in 8 patients with chronic total occlusion (CTO) while analyzing the role of miR-146b-5p in cardiac fibrosis and remodeling after myocardial infarction [16]. It is noteworthy that CTO patients constitute a particular and severe subtype of CAD, which may limit their representativeness in CAD-related research. Moreover, a meta-analysis study aiming to identify differentially expressed miRNAs in the plasma of CAD patients also support the upregulation of miR-146b-5p in the CAD group [30]. Our investigation distinguished itself from prior studies by enrolling a substantially larger cohort of subjects.

Building upon the established upregulation of miR-146b-5p expression in PBMCs, we delved deeper into the correlation between miR-146b-5p and the occurrence and severity of CAD. Furthermore, a study had indicated a gender-specific difference in the renal and cardiac pathological alterations associated with miR-146b-5p [31]. Consequently, we performed a subgroup analysis stratified by sex to further investigate this phenomenon. The subgroup analysis indicated that the expression of miR-146b-5p was significantly higher in CAD patients compared to non-CAD patients, irrespective of gender. This may be partly attributed to the heterogeneity between humans and mice. In addition, they focused on the cardiorenal pathological changes induced by chronic kidney disease models, which did not align with the characteristics of real-world populations.

In this study, three classification strategies were utilized to define the severity of CAD. Initially, based on the traditional categorization of CAD, we observed that the expression of miR-146b-5p was higher in PBMCs of patients with ACS compared to those with SAP. However, further analysis revealed that the levels of miR-146b-5p in MI patients were lower than those in UA, although the difference did not reach statistical significance. This finding aligns with findings from a previous study about miR-146a-5p [32]. From our perspective, it's plausible that the role of miR-146b-5p is more complex than merely being a marker of disease severity. The Gensini score, which is based on the degree of luminal narrowing and the geographic importance of the coronary artery segments involved, is a widely recognized scoring system used to assess the severity of CAD. A weak positive correlation between the Gensini score and miR-146b-5p was observed, prompting that the miR-146b-5p levels may be related to the severity of the lesion to some extent. Of note, SYNTAX score is another comprehensive angiographic tool to assess the complexity of CAD, guide clinical decision-making, and predict the predicting adverse cardiovascular events [33]. Owing to constraints in the availability of data, we refrained from employing this scoring system, which necessitates the evaluation of a multitude of factors, including coronary artery dominance, the number of lesions, lesion location, lesion characteristics, and the presence of chronic total occlusions. In addition, the increased miR-146b-5p level in patients with MVD than those with SVD, further indicating the correlation between miRNA expression and the severity of CAD.

Over the past two decades, as the functions of miRNAs in the pathophysiology of cardiovascular diseases have been increasingly elucidated, numerous studies have found that miRNA can serve as potential biomarkers to guide the diagnosis, treatment, and prognostic assessment of cardiovascular diseases. miR-221 is significantly upregulated in patients with CAD and is involved in various cellular biological processes, including cell proliferation and apoptosis [34]. Yao et al. revealed that miR-221, in conjunction with miR-19b-5p and miR-25-5p, exhibits significant dysregulation in CAD patients presenting with heart failure. The combination of these miRNAs within PBMCs and the presence of hypertension exhibited a strong link to a heightened risk of HF among individuals with CAD [35]. The combination of miRNA and AI is also expected to play a significant role in the diagnosis and treatment of complex CAD and their comorbidities [36]. In our study, ROC analysis demonstrated that miR-146b-5p exhibited good sensitivity and specificity, indicating that miR-146b-5p has the potential to distinguish between CAD and non-CAD.

It has been reported that miR-146b-5p, an endotoxin-responsive noncoding RNA, could respond to a series of inflammatory stimuli and is intimately associated with the TLR-NF- κ B signaling pathway. TLR signaling is usually activated by many cytokines, such as pathogen-derived molecules, endogenous ligands, environmental factors, et al. [37]. Subsequently, the assembly of IRAK and TRAF into a signalosome complex triggers the downstream signaling cascades of the innate immune response, thereby activating NF- κ B. The canonical NF- κ B activation pathway also involves the phosphorylation and subsequent degradation of I κ B proteins under the mediation of the IKK complex, allowing NF- κ B dimers to translocate to the nucleus, further promoting the inflammatory cascade reaction in cells. MiR-146b is involved in the TLR signaling pathways via binding to the 3'UTR of TRAF6 and IRAK1 which are the downstream molecules of TLR4 [38]. Transcription factor interferon regulatory factor 5 (IRF5) is integral to the gene induction program activated by TLRs, which is crucial for the production of pro-inflammatory cytokines. Peng L et al. pointed out that miR-146b was involved in IL 10-induced anti-inflammatory reaction by targeting IRF5, and further inhibited M1 macrophage activation in acute kidney injury [39]. In addition, the enhanced transcription of miR-146b-5p under conditions of stress or hypoxia was found to be dependent on NF- κ B signaling, suggesting there is a negative feedback regulation of miR-146b-5p and NF- κ B signaling [16]. Therefore, the higher expression of miR-146b-5p in CAD patients and its function in THP-1 cells is understandable in this study. Notably, several literatures found the opposite functions of miR-146b-5p in different cell types or under varying stress conditions, indicating that miR-146b-5p, as a reactive non-coding RNA, may exhibit distinct roles at different stages of disease and participate in complex feedback mechanisms. In our study, we predicted and verified that miR-146b-5p could bind to the 3'UTR of IKK β , an important component of IKK complex, and suppress IKK β expression in macrophages, which further enrich the close feedback relationship between miR-146b-5p and NF- κ B pathway.

Although miRNAs have shown potential as therapeutic targets and biomarkers for cardiovascular disease, miRNA-based therapeutic agents have not yet been successfully applied in clinical settings. Challenges in translating miRNAs to clinical use are indisputable. Initially, miRNAs' ability to bind multiple genes complicates the precise elucidation of their functional roles. Even with sophisticated algorithms and databases which aid in predicting binding sites, the exact functions of many miRNAs are still ambiguous and not consistently verifiable across different biological settings. Furthermore, off-target effect is another challenge due to the poly-specificity of miRNAs, which potentially triggering adverse

responses. Moreover, ensuring effective delivery of miRNAs is crucial for their functionality. While delivery systems such as lipid nanoparticles (LNPs) have proven effective for siRNA and mRNA vaccines, miRNA therapy confronts more significant delivery obstacles [40].

Our study has some limitations. Primarily, the single-center cross-sectional design, while effective in identifying a significant association between miR-146-5p and CAD, may not adequately capture the diversity of the broader patient population. The correlation we observed merits further scrutiny with a more extensive and varied participant base, potentially through multi-center studies, to enhance the external validity of our findings. Secondly, several risk assessment tools have previously been employed to evaluate the long-term risks associated with cardiovascular diseases. For instance, the Intermountain Risk Score (IMRS) is utilized to assess the risk of heart failure and sudden cardiac death following STEMI, while the Naples Score is designed to predict long-term outcomes in patients with STEMI [41, 42]. However, these scoring systems primarily rely on basic patient characteristics and biochemical markers. The incorporation of miR-146b-5p measurements may potentially provide a new perspective to enhance the prognostic value of these assessments. Subsequent long-term follow-up study to more thoroughly analyze the value of miR-146b-5p in assessing the prognosis of patients with CAD is necessary. Thirdly, our functional analysis of miR-146-5p is limited to in vitro cellular studies. Future work should aim to extend these findings to animal models to substantiate the cellular observations. Moreover, our investigation into the mechanisms of miR-146-5p action is relatively cursory. A more comprehensive investigation into the molecular pathways is necessary to elucidate the specific mechanisms by which miR-146-5p influences CAD.

In conclusion, our research revealed the expression of miR-146b-5p in a relatively large sample of the CAD population and conducted preliminary investigations into its function and underlying mechanisms in vitro, which may contribute to the development of novel biomarkers for the diagnosis and prognosis of CAD.

Abbreviations

ACS	Acute coronary syndrome
BMI	Body mass index
CAAD	Coronary artery aneurysmal disease
CAD	Coronary artery disease
CCND1	Cyclin D1
CEACAM1	Carcinoembryonic antigen related cell adhesion molecule 1
CRISPR	Clustered Regularly Interspaced Short Palindromic Repeats
eGFR	Estimated Glomerular Filtration Rate
ELISA	Enzyme-linked immunosorbent assay
HDL-C	High-density lipoprotein cholesterol
IKKB	Inhibitory kappa B kinase beta
IRAK1	Interleukin 1 receptor associated kinase 1
IRF	Interferon regulatory factor
KEGG	Kyoto Encyclopedia of Genes and Genomes

LDL-C	Low-density lipoprotein cholesterol
MI	Myocardial infarction
miRNA	MicroRNA
MVD	Multivessel disease
NF- κ B	Nuclear factor kappa-B
PBMC	Peripheral blood mononuclear cell
qRT-PCR	Quantitative reverse transcription polymerase chain reaction
RIP	RNA binding protein immunoprecipitation assay
ROC	Receiver operating characteristic
STEMI	ST elevation myocardial infarction
SVD	Single vessel disease
TLR	Toll-like receptor
TRAF6	TNF receptor-associated factor 6
UA	Unstable angina
UTR	Untranslated regions
VSMCs	Vascular smooth muscle cells

Supplementary Information

The online version contains supplementary material available at <https://doi.org/10.1186/s12872-025-04530-0>.

Supplementary Material 1

Supplementary Material 2

Acknowledgements

It is not applicable.

Author contributions

XZM and JTY designed and wrote the main manuscript text. XZM, S.M, and Y.H wrote and discussed the methodology. Y.H, Q.W, L.Z, ZYC, QSL, Y.W, and JTY performed the study's data processing and supervision. JTY gave the research fund support. All authors read and approved the final manuscript.

Funding

This work was funded by grants from the National Natural Science Foundation of China (Grant number: 82170392) and Hubei Key Research and Development Program (No. 2021BCA121).

Data availability

The data and materials generated and analyzed during the current study are not publicly available due to patient privacy but are available from the corresponding author upon request.

Declarations

Ethics approval and consent to participate

The study was conducted in accordance with the Declaration of Helsinki and approved by the Tongji Hospital Ethics Committee (ID: TJ-C20140716). Informed consent was obtained from all subjects involved in the study. The animal experiment adhered to the Institutional Animal Care and Use Committee (IACUC) protocols and granted approval by the Animal Research Committee's Ethics Board of Tongji Medical College, Huazhong University of Science and Technology ([2022] IACUC Number 3836). Informed consent was obtained from S.M. for the use of the artery tissue.

Consent for publication

It is Not applicable.

Competing interests

The authors declare no competing interests.

Clinical trial number

Not applicable.

Received: 1 November 2024 / Accepted: 28 January 2025

Published online: 05 February 2025

References

- Sutton NR, Banerjee S, Cooper MM, Arbab-Zadeh A, Kim J, Arain MA, Rao SV, Blumenthal RS. Coronary artery disease evaluation and management considerations for high risk occupations: commercial vehicle drivers and pilots. *Circ Cardiovasc Interv.* 2021;14:e009950.
- Sun J, Qiao Y, Zhao M, Magnussen CG, Xi B. Global, regional, and national burden of cardiovascular diseases in youths and young adults aged 15–39 years in 204 countries/territories, 1990–2019: a systematic analysis of global burden of disease study 2019. *BMC Med.* 2023;21:222.
- Kufazvinei TTJ, Chai J, Boden KA, Channon KM, Choudhury RP. Emerging opportunities to target inflammation: myocardial infarction and type 2 diabetes. *Cardiovasc Res.* 2024;120:1241–52.
- Vergallo R, Liuzzo G. Weekly journal scan: the prognostic value of coronary inflammation in patients with non-obstructive coronary artery disease. *Eur Heart J.* 2024;45:3311–3313.
- Ridker PM, Bhatt DL, Pradhan AD, Glynn RJ, MacFadyen JG, Nissen SE, Prominent R-I, Investigators S. Inflammation and cholesterol as predictors of cardiovascular events among patients receiving statin therapy: a collaborative analysis of three randomised trials. *Lancet.* 2023;401:1293–301.
- Everett BM, MacFadyen JG, Thuren T, Libby P, Glynn RJ, Ridker PM. Inhibition of interleukin-1beta and reduction in atherothrombotic cardiovascular events in the CANTOS trial. *J Am Coll Cardiol.* 2020;76:1660–70.
- Nidorf SM, Fiolet ATL, Mosterd A, Eikelboom JW, Schut A, Opstal TSJ, The SHK, Xu XF, Ireland MA, Lenderink T, Latchem D, Hoogslag P, Jerzewski A, Nierop P, Whelan A, Hendriks R, Swart H, Schaap J, Kuijper AFM, van Hessem MWJ, Saklani P, Tan I, Thompson AG, Morton A, Judkins C, Bax WA, Dirksen M, Alings M, Hankey GJ, Budgeon CA, Tijssen JGP, Cornel JH, Thompson PL and LoDoCo2 trial I. Colchicine in patients with chronic coronary disease. *N Engl J Med.* 2020;383:1838–47.
- Diener C, Keller A, Meese E. Emerging concepts of miRNA therapeutics: from cells to clinic. *Trends Genet.* 2022;38:613–26.
- Samadishadlou M, Rahbarghazi R, Piryaeei Z, Esmaili M, Avci CB, Bani F, Kavousi K. Unlocking the potential of microRNAs: machine learning identifies key biomarkers for myocardial infarction diagnosis. *Cardiovasc Diabetol.* 2023;22:247.
- Iwańczyk S, Lehmann T, Cieśliewicz A, Malesza K, Woźniak P, Hertel A, Krupka G, Jagodziński PP, Grygier M, Lesiak M, Araszkievicz A. Circulating miRNA-451a and miRNA-328-3p as potential markers of coronary artery aneurysmal disease. *Int J Mol Sci.* 2023;24.
- Nguyen MA, Hoang HD, Rasheed A, Duchez AC, Wyatt H, Cottee ML, Graber TE, Sussler L, Robichaud S, Berber I, Geoffrion M, Ouimet M, Kazan H, Maegdefessel L, Mulvihill EE, Alain T, Rayner KJ. miR-223 exerts translational control of proatherogenic genes in macrophages. *Circ Res.* 2022;131:42–58.
- Pedersen OB, Grove EL, Nissen PH, Larsen SB, Pasalic L, Kristensen SD, Hvas AM. Expression of microRNA predicts cardiovascular events in patients with stable coronary artery disease. *Thromb Haemost.* 2023;123:307–16.
- Santa-Inez DC, Fuziwara CS, Saito KC, Kimura ET. Targeting the highly expressed microRNA miR-146b with CRISPR/Cas9n gene editing system in thyroid cancer. *Int J Mol Sci.* 2021;22.
- Bonacini M, Rossi A, Ferrigno I, Muratore F, Boiardi L, Cavazza A, Bisagni A, Cimino L, De Simone L, Ghidini A, Malchiodi G, Corbera-Bellalta M, Cid MC, Zerbini A, Salvarani C, Croci. miR-146a and miR-146b regulate the expression of ICAM-1 in giant cell arteritis. *J Autoimmun.* 2024;144:103186.
- Wang C, Cheng H, Yan F, Zhang H, Zhang J, Li C, Zhao M, Shi D, Xiong H. MicroRNA-146b protects kidney injury during urinary tract infections by modulating macrophage polarization. *mBio.* 2023;14:e0209423.
- Liao Y, Li H, Cao H, Dong Y, Gao L, Liu Z, Ge J, Zhu H. Therapeutic silencing miR-146b-5p improves cardiac remodeling in a porcine model of myocardial infarction by modulating the wound reparative phenotype. *Protein Cell.* 2021;12:194–212.
- Sun D, Xiang G, Wang J, Li Y, Mei S, Ding H, Yan J. miRNA 146b-5p protects against atherosclerosis by inhibiting vascular smooth muscle cell proliferation and migration. *Epigenomics.* 2020;12:2189–204.
- Chen P, Li Y, Li L, Yu Q, Chao K, Zhou G, Qiu Y, Feng R, Huang S, He Y, Chen B, Chen M, Zeng Z, Zhang S. Circulating microRNA146b-5p is superior to C-reactive protein as a novel biomarker for monitoring inflammatory bowel disease. *Aliment Pharmacol Ther.* 2019;49:733–43.
- Rampidis GP, Benetos G, Benz DC, Giannopoulos AA, Buechel RR. A guide for Gensini score calculation. *Atherosclerosis.* 2019;287:181–3.
- Mei S, Ma X, Zhou L, Wuyun Q, Cai Z, Yan J, Ding H. CircSMAD3 represses VSMC phenotype switching and neointima formation via promoting hnRNPA1 ubiquitination degradation. *Cell Prolif.* 2025;58:e13742.
- Babaei M, Chamani E, Ahmadi R, Bahreini E, Balouchnejadmojarad T, Nahrkhalaji AS, Fallah S. The expression levels of miRNAs- 27a and 23a in the peripheral blood mononuclear cells (PBMCs) and their correlation with FOXO1 and some inflammatory and anti-inflammatory cytokines in the patients with coronary artery disease (CAD). *Life Sci.* 2020;256:117898.
- Sanchez-Gomar F, Perez-Quilis C, Leischik R, Lucia A. Epidemiology of coronary heart disease and acute coronary syndrome. *Ann Transl Med.* 2016;4:256.
- Takahashi Y, Satoh M, Minami Y, Tabuchi T, Itoh T, Nakamura M. Expression of miR-146a/b is associated with the toll-like receptor 4 signal in coronary artery disease: effect of renin-angiotensin system blockade and statins on miRNA-146a/b and toll-like receptor 4 levels. *Clin Sci (Lond).* 2010;119:395–405.
- Dweep H, Gretz N. miRWalk2.0: a comprehensive atlas of microRNA-target interactions. *Nat Methods.* 2015;12:697.
- Li Q, Verma IM. NF-kappaB regulation in the immune system. *Nat Rev Immunol.* 2002;2:725–34.
- Pelletier D, Rivera B, Fabian MR, Foulkes WD. miRNA biogenesis and inherited disorders: clinico-molecular insights. *Trends Genet.* 2023;39:401–14.
- Jia M, Shi Y, Li Z, Lu X, Wang J. MicroRNA-146b-5p as an oncomiR promotes papillary thyroid carcinoma development by targeting CCDC6. *Cancer Lett.* 2019;443:145–56.
- Yu C, Zhang L, Luo D, Yan F, Liu J, Shao S, Zhao L, Jin T, Zhao J, Gao L. MicroRNA-146b-3p promotes cell metastasis by directly targeting NF2 in human papillary thyroid cancer. *Thyroid.* 2018;28:1627–41.
- Chang TY, Tsai WC, Huang TS, Su SH, Chang CY, Ma HY, Wu CH, Yang CY, Lin CH, Huang PH, Cheng CC, Cheng SM, Wang HW. Dysregulation of endothelial colony-forming cell function by a negative feedback loop of circulating miR-146a and-146b in cardiovascular disease patients. *PLoS ONE.* 2017;12:e0181562.
- Liu L, Zhang J, Wu M, Xu H. Identification of key miRNAs and mRNAs related to coronary artery disease by meta-analysis. *BMC Cardiovasc Disord.* 2021;21:443.
- Paterson MR, Geurts AM, Kriegel AJ. miR-146b-5p has a sex-specific role in renal and cardiac pathology in a rat model of chronic kidney disease. *Kidney Int.* 2019;96:1332–45.
- Zhelankin AV, Stonogina DA, Vasiliev SV, Babalyan KA, Sharova EI, Doludin YV, Shchekochikhin DY, Generozov EV and Akselrod AS. Circulating extracellular miRNA analysis in patients with stable CAD and acute coronary syndromes. *Biomolecules.* 2021;11.
- Hayıroğlu M, Keskin M, Uzun AO, Bozbeyoğlu E, Yıldırım Ö, Kozan Ö, Pehlivanoğlu S. Predictive value of SYNTAX score II for clinical outcomes in cardiogenic shock underwent primary percutaneous coronary intervention; a pilot study. *Int J Cardiovasc Imaging.* 2018;34:329–36.
- Lutfu Askin OT. Is the microRNA-221/222 cluster ushering in a new age of cardiovascular diseases? *Cor et Vasa.* 2023;65:65–7.
- Yao Y, Song T, Xiong G, Wu Z, Li Q, Xia H, Jiang X. Combination of peripheral blood mononuclear cell miR-19b-5p, miR-221, miR-25-5p, and hypertension correlates with an increased heart failure risk in coronary heart disease patients. *Anatol J Cardiol.* 2018;20:100–9.
- Hayıroğlu M, Altay S. The role of artificial intelligence in coronary artery disease and atrial fibrillation. *Balkan Med J.* 2023;40:151–2.
- Luo S, Liao C, Zhang L, Ling C, Zhang X, Xie P, Su G, Chen Z, Zhang L, Lai T, Tang J. METTL3-mediated m6A mRNA methylation regulates neutrophil activation through targeting TLR4 signaling. *Cell Rep.* 2023;42:112259.
- Park H, Huang X, Lu C, Cairo MS, Zhou X. MicroRNA-146a and microRNA-146b regulate human dendritic cell apoptosis and cytokine production by targeting TRAF6 and IRAK1 proteins. *J Biol Chem.* 2015;290:2831–41.
- Peng L, Zhang H, Hao Y, Xu F, Yang J, Zhang R, Lu G, Zheng Z, Cui M, Qi CF, Chen C, Wang J, Hu Y, Wang D, Pierce S, Li L, Xiong H. Reprogramming macrophage orientation by microRNA 146b targeting transcription factor IRF5. *EBioMedicine.* 2016;14:83–96.
- Paunovska K, Loughrey D, Dahlman JE. Drug delivery systems for RNA therapeutics. *Nat Rev Genet.* 2022;23:265–80.
- Mert İlker H, Faysal S, Ahmet Çağdaş Y, Murat S, Tufan Ç. Prognostic value of intermountain risk score for short- and long-term mortality in patients with cardiogenic shock. *Coron Artery Dis.* 2023;34:154–9.

42. Şaylık F, Çınar T, Selçuk M, Akbulut T, Hayiroğlu M, Tanboğa İH. Evaluation of Naples score for long-term mortality in patients with ST-segment elevation myocardial infarction undergoing primary percutaneous coronary intervention. *Angiology*. 2024;75:725–33.

Publisher's note

Springer Nature remains neutral with regard to jurisdictional claims in published maps and institutional affiliations.